



# Study on lawsone derivatives and PVC-modified with lawsone moieties as chemosensors for the detection of nitro-explosives as well as Fe<sup>3+</sup>

Aqeel M.K. Altobee<sup>a</sup> , Wahab K.A. Al-Ithawi<sup>ab</sup> , Leila K. Sadieva<sup>a</sup> , Artem V. Baklykov<sup>ac</sup>, Vadim A. Platonov<sup>a</sup> , Anastasia S. Alekseeva<sup>a</sup>, Alexandra S. Markina<sup>a</sup>, Margarita A. Ereemeeva<sup>d</sup>, Igor S. Kovalev<sup>a</sup>, Dmitry S. Kopchuk<sup>ac</sup> , Grigory V. Zyryanov<sup>ac\*</sup>

**a:** Ural Federal University , Ekaterinburg 620009, Russia

**b:** University of Technology-Iraq , Baghdad 10066, Iraq

**c:** I. Ya. Postovsky Institute of Organic Synthesis , Ekaterinburg 620009, Russia

**d:** South Ural State University , Chelyabinsk, 454080, Russia

\* Corresponding author: [g.v.zyryanov@urfu.ru](mailto:g.v.zyryanov@urfu.ru)

## Abstract

Lawsone and its derivatives have a variety of applications in the field of pharmaceutical research: as drug candidates, reagents for the chelation and recognition of metal cations (including those for catalytic applications), chemosensors for anions, and materials for energy storage applications. Moreover, there are some reports on the application of lawsone and its derivatives in the forensic science field. One of the most attractive features of lawsones is their bright color and well-pronounced fluorescence, which can be altered due to covalent or non-covalent interactions with various species. In this work, we endeavor to present our recent findings on the fluorescence response of lawsone and its methyl ester to nitro compounds and explosives components, such as 2,4-dinitrotoluene (DNT), 2,4,6-trinitrotoluene (TNT), 2,4,6-trinitrophenole (picric acid, PA), 2-nitromesitylene (2-NM), 4-nitrophenol (NP) as well as Fe<sup>3+</sup> (FeCl<sub>3</sub>). In all the cases a dramatic fluorescence *turn-off* response was observed with up to 10<sup>4</sup> M<sup>-1</sup> quenching constants. To explore the practical application of lawsone derivatives a mechanochemical modification of polyvinyl chloride (PVC) with lawsone residues was carried out, and thus obtained polymer was found to exhibit a pronounced fluorescence *turn-off* response to the both nitro-compounds and Fe<sup>3+</sup> with as high as 10<sup>4</sup> M<sup>-1</sup> quenching constants.

## Key findings

- Modification of PVC with lawsone residues under ball-milling conditions was carried out.
- Fluorescence response of lawsone, lawsone methyl ester and lawsone-appended PVC towards DNT, TNT, PA, NP, 2-NM was studied and up to 10<sup>4</sup> M<sup>-1</sup> quenching constants were obtained.
- Fluorescence response of lawsone, lawsone methyl ester and lawsone-appended PVC towards Fe<sup>3+</sup> was studied and up to 10<sup>4</sup> M<sup>-1</sup> quenching constants were obtained.

© 2026, the Authors. This article is published in open access under the terms and conditions of the Creative Commons Attribution (CC BY) license (<http://creativecommons.org/licenses/by/4.0/>), which permits unrestricted reuse of the work in any medium provided the original work is properly cited.

## Accompanying information

### Article history

Received: 27.03.2026

Revised: 22.04.2026

Accepted: 27.04.2026

Available online: 27.04.2026

### Keywords

Lawsone; PVC; ball-milling; fluorescence *turn-off* response; nitro compounds

### Funding

This work was supported by the Russian Science Foundation (grant no. 25-73-30016).

### Supplementary information

Supplementary materials:

Transparent peer review:

### Sustainable Development Goals



## 1. Introduction

Lawsone is a natural dye, which present in the leaves of the henna plant (*Lawsonia inermis*). Lawsone and its derivatives are known by their wide range biological activities [1-

2], as valuable synthon for organic synthesis [3], as well as a material for energy storage applications [4-6]. According to recent research, lawsone has great potential for the application in the forensic science field. In particular, similar to ninhydrin, the mostly used reagent for latent fingerprint

development, lawsone shows similar behavior in recognizing primary amino acids. Lawsone non-specifically targets primary amino acids, and displays strong photoluminescence upon illumination with forensic light sources. [7]. Thus, according to a literature [7] lawsone exhibits a characteristic purple/brown coloration as opposed to the purple/blue coloration developed upon interaction with ninhydrin. And the photoluminescence of lawsone is maximized at 640 nm, which is high enough that it avoids background interference common for ninhydrin [8]. Another application of lawsone and its derivatives for the application in the forensic science field is in the such fact as these 1,4-naphthoquinones are structurally related to naphthalene and its derivative, which are commonly used for the photoluminescence-based explosives detection [9-12].

To the best of our knowledges no reports were published so far on utilization of lawsone and its derivatives for the photoluminescent explosives detection.

In this manuscript we wish to report our studies on the using of lawsone, its methyl ester as well as lawsone-appended PVC as promising chemosensors for the fluorescence *turn-off* detection of nitrocompounds/explosives components.

## 2. Experimental part

All reagents were purchased from commercial sources and used without further purification. NMR spectra were recorded on a Bruker Avance-400 spectrometer, at 298 K, with the digital resolution of  $\pm 0.01$  ppm, using TMS as an internal standard. Ball-milling experiments were carried out on a Retsch PM 100 CM ball mill in 25 mL stainless still milling jar loaded with 4 stainless still milling balls of 10 mm diameter. FT-IR spectra were measured using a LUMOS-Bruker IR-Fourier spectrometer in KBr pellets. GPC measurements were carried out on an Agilent 1200 chromatograph with an evaporative light scattering detector (ELSD) (Agilent technologies, USA). UV-Vis absorption, emission and excitation spectra were obtained and titration experiments were carried out on a Solar CM2203 spectrofluorometer (Belarus). The DFT calculations for lawsone derivatives **1-2** and for nitrocompounds were carried out at the B97-3c level of DFT theory using ORCA 6.1 QC package [13]. As for all structures, positive vibrational frequencies were exclusively obtained, all results shown in this manuscript refer to true minimum energy geometries.

### 2.1. Synthesis of lawsone methyl ether (2-methoxy-1,4-naphthoquinone) (2)

Potassium carbonate (79.5 mg, 0.58 mmol) was added to a solution of lawsone (100 mg, 0.58 mmol) in 4 mL *N,N*-dimethyl formamide. The mixture was stirred at room temperature for 15 min. After addition of methyl iodide (0.085 g, 0.58 mmol), the reaction mixture was further stirred for additional 72 h. When the reaction completed, distilled wa-

ter (30 mL) was added to the reaction mixture and the product was extracted by ethyl acetate (3 × 30 mL). The combined organic phases were dried over anhydrous sodium sulfate and concentrated under reduced pressure. The residue was suspended in methanol (20 mL), and the precipitate formed was filtered, washed with methanol (3×5 mL) and air-dried for 24 hours to give target product.

M.P. = 183-185 °C (ref. [14] 183 °C. NMR <sup>1</sup>H (400 MHz, CDCl<sub>3</sub>,  $\delta$ , ppm): 3.94 (s, 3H), 6.21 (s, 1H), 7.72-7.80 (m, 2H), 8.11 - 8.12 (m, 1H), 8.15-8.16 (m, 1H). NMR <sup>13</sup>C (100 MHz, CDCl<sub>3</sub>,  $\delta$ , ppm) 184.8, 180.1, 160.4, 134.3, 134.2, 133.3, 132.0, 131.0, 126.8, 126.2, 109.8, 56.4. IR (KBr),  $\nu$ , cm<sup>-1</sup>: IR (KBr) cm<sup>-1</sup>: 1680 (C = O), 1645 (C = O), 1605 (C = C, Ar), 1240 (C - O). Found, C 70.01, H 4.33. Calculated for C<sub>11</sub>H<sub>8</sub>O<sub>3</sub>, C 70.21, H 4.29.

### 2.2. Mechanochemical synthesis of lawsone-appended polymer (3)

A 25 mL stainless steel milling jar with 4 g stainless still milling balls (d = 10 mm) was charged with lawsone (87 mg, 0.50 mmol), polyvinyl chloride (0.1 g), K<sub>2</sub>CO<sub>3</sub> (0.14 g, 1 mmol), and 2 drops of cyclohexanone. The mixture was stirred for 4 h at 500 rpm.

The resulting reaction mixture was suspended in a methanol:water mixture = 2:1 (50 mL), the resulting suspension was filtered, the precipitate was washed with water (3 × 5 mL), and dried. Then the precipitate was suspended in methanol (60 ml) containing KOH (0.18 g, 3 mmol) and boiled for 3 h.

The resulting precipitate was filtered, washed with water (3 × 5 ml), methanol (3 × 5 ml), and dried for 24 h at room temperature.

**Polymer (3)**. Off-white solid. Yield 0.12 g (53%). NMR <sup>1</sup>H (400 MHz, DMF-d<sub>7</sub>,  $\delta$ , ppm): 2.33-2.59 (m, 2H), 4.49-4.65 (m, 1H), 5.54 (s, 1H), 7.45-7.48 (m, 1H), 7.62-7.65 (m, 1H), 7.93-7.96 (m, 1H), 8.02-8.06 (m, 1H). IR (KBr),  $\nu$ , cm<sup>-1</sup>: 1648 (C=O), 1251 (C-O). GPC (DMF), M<sub>n</sub> = 197 kDa (PDI= 1.4).

## 3. Results and discussion

Naphthalene derivatives are well known to possess strong fluorescence and these compounds [9-11] and materials bearing naphthalene units [12] are widely used for the fluorescence turn-off detection of nitro-compounds. Lawsone (2-hydroxy-1,4-naphaquinone) contains electron-donating 2-hydroxygroup and in theory it may interact with electron-deficient species. Thus, lawsone-based complexes with metal cations are widely reported [15-17]. And the formation of stable lawsone anions upon interaction with metal cations/ammonium salts was confirmed by X-ray data [18].

To study the possibility lawsone interaction with electron-deficient nitro-compounds, lawsone **1** isolated from natural source was used and two lawsone derivatives were

prepared. As a first step by means of *O*-alkylation of 2-hydroxygroup in **1** were carried out by means of reaction with methyl iodide in DMF at room temperature to produce 2-methoxy-1,4-naphthoquinone **2** in 79% yield (Scheme 1).

In addition, we have prepared a lawsone-appended polyvinyl chloride (PVC) **3** by means of reaction between **1** and commercially available polyvinyl chloride under ball-milling conditions at 500 rpm for 4 hours in the presence of potassium carbonate, which was used both as a base and as an additional abrasive. Structures of lawsone derivative **2** and lawsone-appended PVC **3** were confirmed by means of set of physical methods. Thus, <sup>1</sup>H NMR spectra of **2** (Figures S1–S2) and **3** (Figure S3) contain resonance signals of the protons of the aromatic fragments of 1,4-naphthoquinone as multiplets in the range of 7.46–8.06 ppm, a resonance signal of the proton at the C3 atom as a singlet in the region of 5.54 ppm and resonance signals of the protons of methyl and PVC fragments, namely as three proton singlet next to 3.50 ppm (in case of compound **2**) or multiplets in the regions of 2.33–2.59 and 4.49–4.65 ppm (in case of polymer **3**) (Figures S1–S3). According to the <sup>1</sup>H NMR data, the degree of modification of PVC with the lawsone fragment in polymer **3** reaches 8%. The IR spectrum of polymer **3** contains absorption bands of the C=O (1648 cm<sup>-1</sup>), C–O (1254 cm<sup>-1</sup>), and C–H (2966 cm<sup>-1</sup>) groups, but no absorption band of the OH group (~3400 cm<sup>-1</sup>). All this indicates *O*-alkylation of the phenolic group at the C2 atom of naphthoquinone in the both cases. In addition gel permeation chromatography experiments were carried out, and the number-average mass of the polymer **3** equal to M<sub>n</sub> = 197 kDa was calculated with polydispersity index PDI = 1.4.

As a next step photophysical studies of lawsone derivatives **1–3** were carried out. Thus, in DMF solutions in absorption spectra of compound **1–3** three absorption bands were detected (Figure 1A), but methyl-lawsone **2** lacks one long wavelength broad band. In emission spectra (Figure 1B) in all the cases all lawsone derivatives are to show similar trend with similar vibronic shape of emission peaks. In DMF solutions all three compounds emit in a similar blue region (high intensity emission bands at ~ 400–450 nm) as well as in orange-red region (low intensity emission bands at ~ 675 nm). Remarkable, that those of methylated lawsone **2** is red-shifted relative to lawsone **1** and polymer **3** and has the most prominent vibronic structure with three maxima. It worth to mention, that lawsone derivatives **1–3** in DMF emit in shorter wavelength region compared to literature data registered in ethanol [19,20]. It should be noted, that in case of polymer **3** the obtained results are to confirm the introduction of lawsone moiety in PVC core.

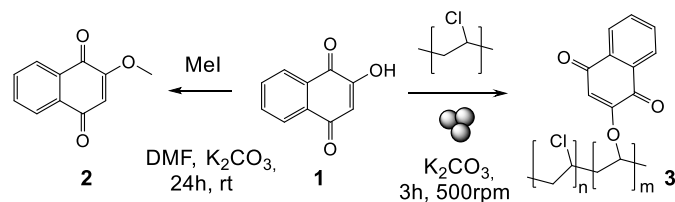
As a next step, the fluorescence response of lawsone derivatives **1–2** towards nitro-compounds, such as DNT, TNT, PA, PETN (pentaerythritol tetranitrate), DMDNB (2,3-dimethyl-2,3-dinitrobutane), NB (nitrobenzene), NP and 2-NM was studied in solution. Based on the results of DFT calculations the values of LUMO energy levels of lawsone

derivatives **1–2** are higher than LUMO energy levels of TNT and PA (Table S1) to provide an efficient fluorescence quenching via PET process. Upon addition of DNT, TNT, PA, 2-NM and NP a dramatic quenching of fluorescence took place (Figures 2–3, Figures S5–S12, S14–S21 Table S2), which confirms strong fluorescence “turn-off” response of lawsone derivatives **1–2** towards nitro compounds. In Stern-Volmer plots a good linearity of graphs took place. It worth to mention that no shifts of emission maxima were observed, which suggests false static quenching mechanism.

The fluorescence response of all the compounds towards common nitroaromatic quenchers was quantitatively evaluated by calculation of Stern-Volmer quenching constant using the Stern-Volmer static quenching model according to equation (1) and quenching efficiency was quantitatively estimated as:

$$\frac{I_0}{I} = 1 + K_{SV} \times [Q], \quad (1)$$

where I<sub>0</sub> is the intensity of fluorescence in the absence of a quencher, I is the intensity of fluorescence in the presence of a quencher, K<sub>SV</sub> is the Stern-Volmer quenching constant for complex formation, and [Q] is the concentration of the quencher.



**Scheme 1**

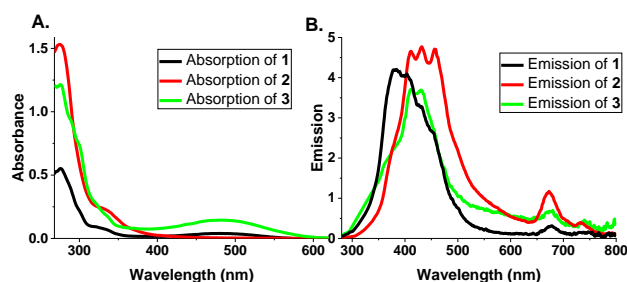


**Figure 1** UV-Vis absorption (A) and emission (B) spectra of compounds **1–3** in DMF

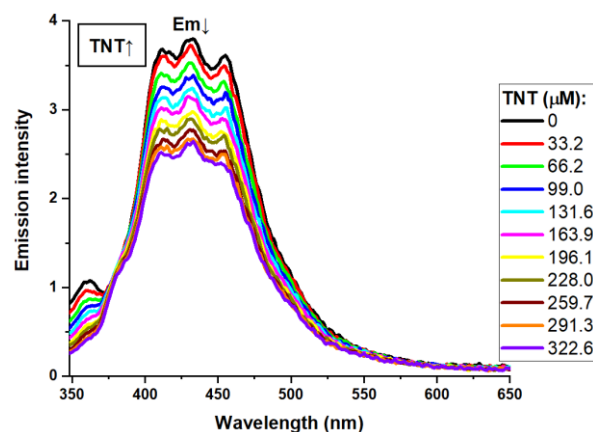


**Figure 2** Fluorescence quenching of lawsone **1** in the presence of TNT. Insert shows Stern-Volmer graph.

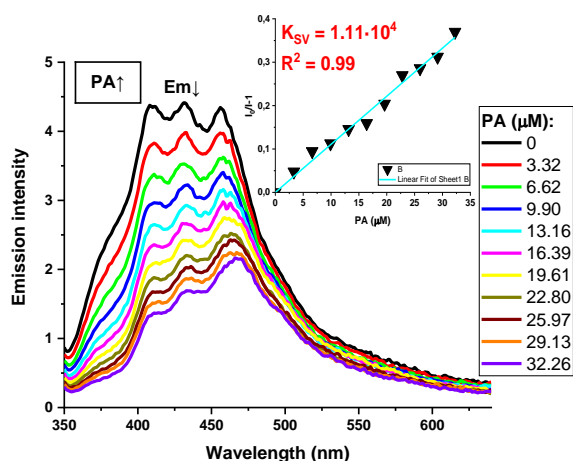


**Figure 3** Fluorescence quenching of *O*-methyl-lawsone **2** in the presence of PA. Insert shows Stern-Volmer graph.

The quenching constant ( $K_{sv}$ ) was calculated as the slope of the graph intensity  $((I_0/I)-1)$  versus the concentration of the quencher ( $[Q]$ ).

$$\text{Quenching efficiency (\%)} = \frac{I_0 - I}{I_0} \times 100, \quad (2)$$

where  $I_0$  is the intensity of fluorescence in the absence of a quencher,  $I$  is the intensity of fluorescence in the presence of a quencher.

The limit of detection (LOD) was determined based on the data from fluorescence quenching experiments in accordance with the method published earlier [21]. To obtain the equation of the regression curve, a calibration graph of the sensor fluorescence intensity versus the analyte concentration was plotted. The limit of detection was calculated using the following equation:

$$\text{LOD} = \frac{3\sigma}{k}, \quad (3)$$

where  $\sigma$  is the standard deviation of the fluorophore intensity in the absence of the analyte obtained using the STEYX function in Excel,  $k$  is the slope of the calibration curve.

To explore a possible practical application of lawsone derivatives in the forensic science field, fluorescence titration studies were carried out for the polymer **3**, and again strong fluorescence turn-off response in case of all above-mentioned nitrocompounds (DNT, TNT, PA, NP, 2-NM) was observed (Figure 4, Figures S23–S30) due to the involvement of lawsone units on the periphery of PVC into the interaction with nitrocompounds. The calculated Stern-Volmer quenching constants were calculated and as high as  $10^4 \text{ M}^{-1}$  values were found with good linearity Stern-Volmer graphs.

As a final step the fluorescence response of lawsone derivatives **1-3** to cations, especially  $\text{Fe}^{3+}$ , which is of wide importance in terms of biological activity [22,23] and environmental impact [24]. Thus, in DMF solutions upon addition of cations to the solutions of **1-3** in DMF a dramatic fluorescence quenching took place in the presence of  $\text{FeCl}_3$  (Figures 5,6, Figures S13, S22, S31–S33) with quenching constants up to  $10^4 \text{ M}^{-1}$ .

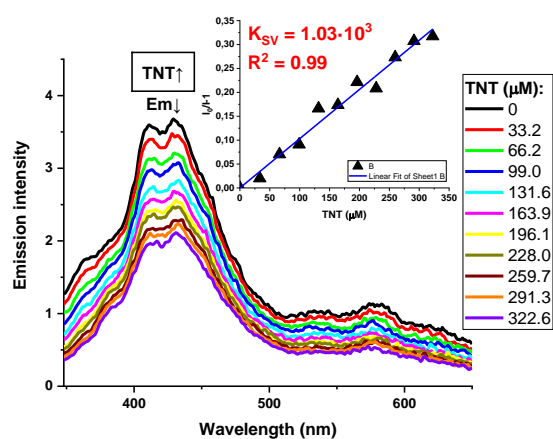


**Figure 4** Fluorescence quenching of polymer **3** in the presence of TNT. Insert shows Stern-Volmer graph

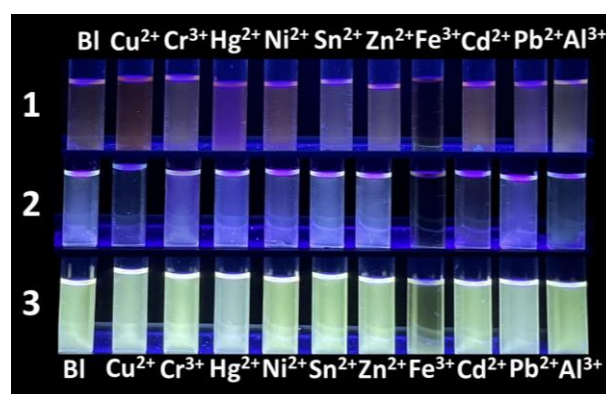


**Figure 5** Qualitative assessment of the presence of cations by compounds **1-3** under 254 nm UV light.

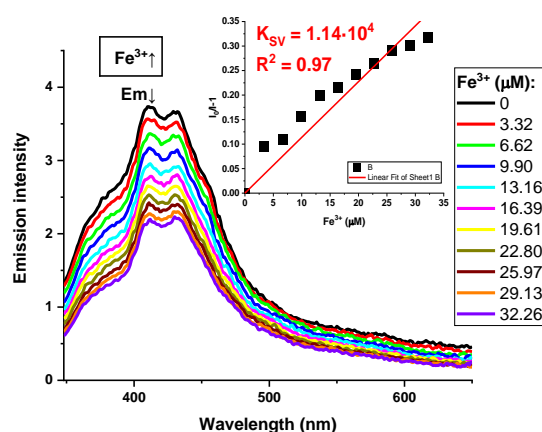


**Figure 6** Fluorescence quenching of polymer **3** in the presence of  $\text{FeCl}_3$ . Insert shows Stern-Volmer graph.

It is well known that fluorescence quenching in the presence of various analytes can be due, among other things as Förster resonance energy transfer (FRET) and photo-induced electron transfer (PET), to the inner filter effect (IFE), if analytes absorb at excitation and emission wavelengths of chemosensors-fluorophores, which is what happens in our case (Figure 7). So, we assumed the possible presence of IFE and decided to investigate this matter more precisely.

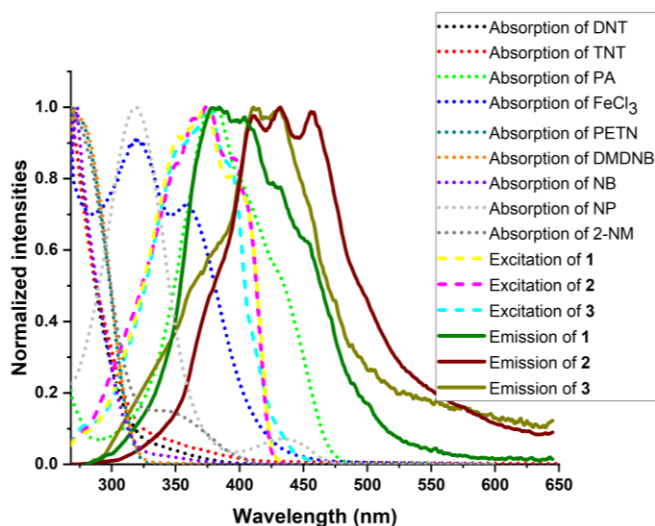


**Figure 7** An overlay of absorption of DNT, TNT, PA, PETN, DMDNB, NB, NP, 2-NM and  $\text{FeCl}_3$ , emission of compounds **1-3** and excitation of compounds **1-3**

**Table 1** Stern-Volmer constants of lawsone derivatives **1-3** in the presence of various quenchers.

Compound	1	2	3
DNT, $\text{M}^{-1}$	$0.58 \cdot 10^3$	–	$2.24 \cdot 10^3$
TNT, $\text{M}^{-1}$	$0.43 \cdot 10^3$	–	$1.03 \cdot 10^3$
PA, $\text{M}^{-1}$	$8.91 \cdot 10^3$	$1.11 \cdot 10^4$	–
PETN, $\text{M}^{-1}$	–	–	–
DMDNB, $\text{M}^{-1}$	–	–	–
NB, $\text{M}^{-1}$	–	–	–
NP, $\text{M}^{-1}$	–	–	$1.23 \cdot 10^4$
2-NM, $\text{M}^{-1}$	$0.24 \cdot 10^3$	–	$0.86 \cdot 10^3$
$\text{FeCl}_3$ , $\text{M}^{-1}$	$1.11 \cdot 10^4$	–	$1.14 \cdot 10^4$

<sup>a</sup>After inner filter effect (IFE) correction.

There are a large number of methods described in the literature for the IFE correction [25]; one among them is Parker's method improved by Lakowicz (4) [26] that we chose as it frequently used in the field of chemosensing [27,28]:

$$F_{\text{corr}} = F_{\text{obs}} \times \text{antilog} \left( \frac{OD_{\text{ex}} + OD_{\text{em}}}{2} \right), \quad (4)$$

where  $F_{\text{corr}}$  и  $F_{\text{obs}}$  are the corrected and observed fluorescence intensities,  $OD_{\text{ex}}$  и  $OD_{\text{em}}$  are the absorption at the excitation and emission wavelengths, respectively.

Corrected fluorescence intensities were used to recalculate Stern-Volmer constant, quenching efficiency values and limit of detection according to Equations (1)–(3) respectively. The obtained corrected data are summarized in the Table 1 and full data are presented in a Tables S2 and S3.

Indeed, all lawsone derivatives **1-3** showed fluorescence *turn-off* response to the presence of both nitro-containing analytes and  $\text{Fe}^{3+}$ , but mechanism differs. Both Stern-Volmer constant and quenching efficiency values just decreased after IFE correction but were not eliminated completely in the case of compound Lawsone for all analytes and in the case of polymer **3** for all analytes except PA, insisting the occurrence of other fluorescence quenching mechanisms. As for compound **2**, it showed non-IFE attributed response only to PA, whereas response of polymer

**3** to the same analyte, on the contrary, was attributed purely to IFE.

## 4. Limitations

Due to low solubility of polymer **3** GPC experiments in THF are failed. Therefore, these studies were carried out in DMF. In the presence of various analytes, fluorescence quenching can be due to the inner filter effect (IFE) if the analytes absorb at the excitation and emission wavelengths of the chemosensor-fluorophores, as is the case here. To exclude the influence of IFE, all of the obtained quenching constants were recalculated.

## 5. Conclusions

In summary, for a first time the possibility of using lawsone and its *O*-methyl-substituted derivative as chemosensors for the fluorescence detection of nitro-compounds, such as 2,4-dinitrotoluene, 2,4,6-trinitrotoluene, picric acid and 2-nitromesitylene in solution was demonstrated. The herein reported lawsone derivatives in the presence of above-mentioned nitro-compounds exhibited dramatic fluorescence *turn-off* response with up to  $10^4 \text{ M}^{-1}$  quenching constants. To explore practical applications the lawsone-appended PVC was prepared by means of mechanosynthesis under ball-milling conditions. This polymer also exhibited a pronounced fluorescence *turn-off* response in the presence of nitro-compounds with up to  $10^4 \text{ M}^{-1}$  quenching constants. In addition, a fluorescence *turn-off* response of lawsone derivatives **1-3** towards  $\text{Fe}^{3+}$  cation was studied and as high as  $10^4 \text{ M}^{-1}$  quenching constants was observed. The herein obtained results are to explore the application of lawsone derivatives in the forensic science field.

## Supplementary materials

**Figure S1:**  $^1\text{H}$  NMR of lawsone methyl ether **2** in  $\text{CDCl}_3$ ; **Figure S2:**  $^1\text{H}$  NMR of lawsone methyl ether **2** in DMF; **Figure S3:**  $^1\text{H}$  NMR of polymer **3** in DMF; **Table S1:** HOMO and LUMO energy levels of nitro-compounds and lawsone derivatives **1-2**; **Figure S4:** Excitation spectra of compounds **1,2** and polymer **3** in DMF; **Table S2:** Summary of photophysical data for compounds **1-3**; **Table S3:** Summary of Stern-Volmer quenching constants ( $K_{\text{sv}}$ ), quenching efficiency (QE) of compounds **1,2** and polymer **3** before and after IFE correction; **Table S4:** Summary of limit of detection (LOD) of compounds **1,2** and polymer **3** after IFE correction; **Table S5:** Excitation and emission wavelengths of compounds **1-3** in fluorescence titration experiments and  $K_{\text{sv}}$  values and IFE correction calculations; **Figure S5:** Overlaid spectra of fluorescence quenching of **1** upon addition of DNT in DMF; insert – Stern-Volmer plot of the fluorescence “turn-off” response of **1** to DNT after inner filter effect (IFE) correction; **Figure S6:** Overlaid spectra of fluorescence quenching of **1** upon addition of TNT in DMF; insert – Stern-Volmer plot of the fluorescence “turn-off” response of **1** to TNT after inner filter effect (IFE) correction; **Figure S7:** Overlaid spectra of fluorescence quenching of **1** upon addition of PA in DMF; insert – Stern-Volmer plot of the fluorescence “turn-off” response of **1** to PA after inner filter effect (IFE) correction; **Figure S8:** Overlaid spectra of fluorescence titration of **1** upon addition of PETN in DMF; **Figure S9:** Overlaid spectra of fluorescence titration of **1** upon addition of DMDNB in DMF; **Figure S10:** Overlaid spectra of fluorescence titration of **1** upon addition of NB in DMF; **Figure S11:** Overlaid spectra of fluorescence quenching of **1** upon addition of NP in DMF; **Figure S12:** Overlaid spectra of fluorescence quenching

of **1** upon addition of 2-NM in DMF; insert – Stern-Volmer plot of the fluorescence “turn-off” response of **1** to 2-NM after inner filter effect (IFE) correction; **Figure S13**: Overlaid spectra of fluorescence quenching of **1** upon addition of Fe<sup>3+</sup> in DMF; insert – Stern-Volmer plot of the fluorescence “turn-off” response of **1** to Fe<sup>3+</sup> after inner filter effect (IFE) correction; **Figure S14**: Overlaid spectra of fluorescence quenching of **2** upon addition of DNT in DMF; **Figure S15**: Overlaid spectra of fluorescence quenching of **2** upon addition of TNT in DMF; **Figure S16**: Overlaid spectra of fluorescence quenching of **2** upon addition of PA in DMF; insert – Stern-Volmer plot of the fluorescence “turn-off” response of **2** to PA after inner filter effect (IFE) correction; **Figure S17**: Overlaid spectra of fluorescence titration of **2** upon addition of PETN in DMF; **Figure S18**: Overlaid spectra of fluorescence titration of **2** upon addition of DMDNB in DMF; **Figure S19**: Overlaid spectra of fluorescence titration of **2** upon addition of NB in DMF; **Figure S20**: Overlaid spectra of fluorescence quenching of **2** upon addition of NP in DMF; **Figure S21**: Overlaid spectra of fluorescence quenching of **2** upon addition of 2-NM in DMF; **Figure S22**: Overlaid spectra of fluorescence quenching of **2** upon addition of Fe<sup>3+</sup> in DMF; **Figure S23**: Overlaid spectra of fluorescence quenching of polymer **3** upon addition of DNT in DMF; insert – Stern-Volmer plot of the fluorescence “turn-off” response of polymer **3** to DNT after inner filter effect (IFE) correction; **Figure S24**: Overlaid spectra of fluorescence quenching of polymer **3** upon addition of TNT in DMF; insert – Stern-Volmer plot of the fluorescence “turn-off” response of polymer **3** to TNT after inner filter effect (IFE) correction; **Figure S25**: Overlaid spectra of fluorescence quenching of polymer **3** upon addition of PA in DMF; **Figure S26**: Overlaid spectra of fluorescence titration of **3** upon addition of PETN in DMF; **Figure S27**: Overlaid spectra of fluorescence titration of **3** upon addition of DMDNB in DMF; **Figure S28**: Overlaid spectra of fluorescence titration of **3** upon addition of NB in DMF; **Figure S29**: Overlaid spectra of fluorescence quenching of **3** upon addition of NP in DMF; insert – Stern-Volmer plot of the fluorescence “turn-off” response of polymer **3** to NP after inner filter effect (IFE) correction; **Figure S30**: Overlaid spectra of fluorescence quenching of **3** upon addition of 2-NM in DMF; insert – Stern-Volmer plot of the fluorescence “turn-off” response of polymer **3** to 2-Nm after inner filter effect (IFE) correction; **Figure S31**: Overlaid emission spectra of compound **1** in the presence of different cations (each cation was added as 100 mL of 32 μM solution); **Figure S32**: Overlaid emission spectra of compound **2** in the presence of different cations (each cation was added as 100 mL of 32 μM solution); **Figure S33**: Overlaid emission spectra of polymer **3** in the presence of different cations (each cation was added as 100 mL of 32 μM solution); **Figure S34**: Overlaid emission spectra of compound **1** in the presence of different cations (each cation was added as 100 mL of 32 μM solution) and nitro-analytes (each nitro-analyte was added as 100 mL of 320 μM solution); **Figure S35**: Overlaid emission spectra of polymer **3** in the presence of different cations (each cation was added as 100 mL of 32 μM solution) and nitro-analytes (each nitro-analyte was added as 100 mL of 320 μM solution); **Figure S36**: Overlaid normalized absorption spectra of analytes (nitro-containing ones and FeCl<sub>3</sub>) and compounds **1-3** in DMF; **Figure S37**: IR-spectra of polymer **3** in KBr. **Figure S38**: IR-spectra of lawsone **1** in KBr. **Figure S39**: IR-spectra of lawsone methyl ether **2** in KBr.

### Data availability statement

The data that support the findings of this study are available on re-request from the corresponding author.

### Acknowledgments

None.

### Author contributions

Conceptualization: G.V.Z.

Data curation: A.M.K.A., W.K.A.A., A.V.B., L.K.S., I.S.K., D.S.K., V.A.P., Y.K.S., A.S.A., A.S.M., M.A.E., G.V.Z.

Formal Analysis: A.M.K.A., W.K.A.A., A.V.B., I.S.K., D.S.K., V.A.P., L.K.S., A.S.A., A.S.M., M.A.E., G.V.Z.

Funding acquisition: G.V.Z.

Investigation: A.M.K.A., W.K.A.A., A.V.B., I.S.K., D.S.K., A.S.A., A.S.M., M.A.E., V.A.P., L.K.S.,

Methodology: A.M.K.A., W.K.A.A., A.V.B., I.S.K., D.S.K., V.A.P., L.K.S.

Project administration: G.V.Z.

Resources: A.V.B., V.A.P., I.S.K., L.K.S.

Software: A.V.B., V.A.P., I.S.K., L.K.S.

Supervision: G.V.Z.

Validation: A.M.K.A., W.K.A.A., A.V.B., I.S.K., D.S.K., V.A.P., L.K.S.

Visualization: G.V.Z.

Writing – original draft: A.M.K.A., W.K.A.A., A.V.B., L.K.S., I.S.K., D.S.K., V.A.P., Y.K.S., A.S.A., A.S.M., M.A.E., G.V.Z.

Writing – review & editing: A.M.K.A., W.K.A.A., A.V.B., I.S.K., D.S.K., V.A.P., L.K.S., A.S.A., A.S.M., M.A.E., G.V.Z.

### Conflict of interest

‘The authors declare no conflict of interest’ or declare any potential (ethical, financial) interests if they exist.

### Additional information

Author Scopus IDs:

Aqeel M.K. Altobee, [59177207900](https://orcid.org/0009-0001-59177207900);

Wahab K. A. Al-Ithawi, [57190679522](https://orcid.org/0009-0001-57190679522);

Artem V. Baklykov, [57205549944](https://orcid.org/0009-0001-57205549944);

Vadim A. Platonov, [57359125100](https://orcid.org/0009-0001-57359125100);

Igor S. Kovalev, [7102090085](https://orcid.org/0009-0001-7102090085);

Dmitry S. Kopchuk, [14123383900](https://orcid.org/0009-0001-14123383900);

Leila K. Sadieva, [57196004979](https://orcid.org/0009-0001-57196004979);

Grigory V. Zyryanov, [6701496404](https://orcid.org/0009-0001-6701496404).

Websites:

Ural Federal University, <https://urfu.ru/en/>;

University of Technology-Iraq, <https://www.uotechnology.edu.iq/>;

I. Ya. Postovsky Institute of Organic Synthesis, <https://www.io-suran.ru/>.

### References

- Dash A, Panda J, Samanta B, Mohapatra S. Advancements in synthetic methodologies and biological applications of lawsonone derivatives. *Org. Biomol. Chem.* 2025;23(10):2302–22. [doi:10.1039/D5OB00020C](https://doi.org/10.1039/D5OB00020C)
- Nair AS, Sekar M, Gan SH, Kumarasamy V, Subramaniyan V, Wu YS, Wong LS. Lawsonone unleashed: A comprehensive review on chemistry, biosynthesis, and therapeutic potentials. *Drug Des. Dev. Ther.* 2024;18:3295–3313. [doi:10.2147/DDDT.S463545](https://doi.org/10.2147/DDDT.S463545)
- Jordao AK, Vargas MD, Pinto AC, da Silva FDC, Ferreira VF. Lawsonone in organic synthesis. *RSC Adv.* 2015;5(83):67909–43. [doi:10.1039/C5RA12785H](https://doi.org/10.1039/C5RA12785H)
- Miroshnikov M, Kato K, Babu G, Divya KP, Arava LMR, Ajayan PM, John G. A common tattoo chemical for energy storage: henna plant-derived naphthoquinone dimer as a green and sustainable cathode material for Li-ion batteries. *RSC Adv.* 2018;8(3):1576–82. [doi:10.1039/C7RA12357D](https://doi.org/10.1039/C7RA12357D)
- Jonson RA, Battaglia VS, Tucker MC. Lithium batteries with small-molecule quinone cathode enabled by lithium garnet separators. *ACS Appl. Energy Mater.* 2023;6(2):745–52. [doi:10.1021/acsaem.2c02932](https://doi.org/10.1021/acsaem.2c02932)
- Gupta R, Ramanujam K. A highly conjugated tetrakis-lawsonone organic cathode material for enhancing the capacity utilization in the zinc-ion batteries. *J. Chem. Sci.* 2024;136(2):19. [doi:10.1007/s12039-023-02244-4](https://doi.org/10.1007/s12039-023-02244-4)
- Jelly R, Lewis SW, Lennard C, Lim KF, Almog J. Lawsonone: a novel reagent for the detection of latent fingerprints on paper surfaces. *ChemComm.* 2008;30:3513–15. [doi:10.1039/b808424f](https://doi.org/10.1039/b808424f)
- Thomas P, Farrugia K. An investigation into the enhancement of fingerprints in blood on paper with genipin and lawsonone. *Sci. Justice.* 2013;53(3):315–20. [doi:10.1016/j.scijus.2013.04.006](https://doi.org/10.1016/j.scijus.2013.04.006)
- Zhu W, Wang C, Li W, Tao CA, Cui J, Yang H, Li G. A new strategy for selective detection of nitrated explosives based

- on a confinement effect of nanocavity. *J. Mater. Chem. A*. 2013;1(38):11741-7. doi:10.1039/C3TA11881A
10. Ghosh P, Das J, Basak A., Mukhopadhyay SK, Banerjee P. Nanomolar level detection of explosive and pollutant TNP by fluorescent aryl naphthalene sulfones: DFT study, in vitro detection and portable prototype fabrication. *Sens. Actuator B-Chem.* 2017;251:985-92. doi:10.1016/j.snb.2017.05.126
  11. Bal M, Köse A, Özpaça Ö, Köse M. Pyrene, anthracene, and naphthalene-based azomethines for fluorimetric sensing of nitroaromatic compounds. *J. Fluoresc.* 2023;33(4):1443-55. doi:10.1007/s10895-023-03155-w
  12. Ahamed S, Bhaumik B, Tohora N, Chourasia J, Lama S, Mahato M, Das SK. Naphthalene-based fluorescent room temperature ionic liquid derived organo-nanosensor for detection of explosive nitroaromatic compounds. *Microchem. J.* 2025;213:113759. doi:10.1016/j.microc.2025.113759
  13. Neese F. Software update: the ORCA program system, version 6.0. *WIREs Comput. Molec. Sci.* 2025;15(1):e70019. doi:10.1002/wcms.70019
  14. Pharkphoom P, Wantana R. Evaluation of Chemical Stability and Skin Irritation of Lawsone Methyl Ether in Oral Base. *Pharm. Biol.* 2002;40(6):429-32. doi:10.1076/phbi.40.6.429.8443
  15. Salunke-Gawali S, Pereira E, Dar UA, Bhand S. Metal complexes of hydroxynaphthoquinones: Lawsone, bis-lawsone, lapachol, plumbagin and juglone. *J. Mol. Struct.* 2017;1148:435-458. doi:10.1016/j.molstruc.2017.06.130
  16. Frontana CE, Valle G, Ugalde-Saldívar VM, González I. Metallic Interaction Effects on the Reactivity of Lawsone Semiquinones. *ECST.* 2007;3(29):93-102. doi:10.1149/1.2753294
  17. Elenen MNA, Elshobaky AR, Elsayed SA. New Silver (I) Lawsone-based complexes: Synthesis, characterization, interaction with biological macromolecules, in vitro antineoplastic, antimetastatic, and antimicrobial activity. *J. Mol. Struct.* 2024;1317:139048. doi: j.molstruc.2024.139048
  18. Salunke-Gawali S, Kathawate L, Shinde Y, Puranik VG, Weyhermüller T. Single crystal X-ray structure of Lawsone anion: evidence for coordination of alkali metal ions and formation of naphthosemiquinone radical in basic media. *J. Mol. Struct.* 2012;1010:38-45. doi:10.1016/j.molstruc.2011.11.015
  19. Giustetto R, Barbero N, Bonino F, Guiotto V, Pontremoli C, Ricchiardi G. Structural and physicochemical properties of Mayan-inspired hybrid nanocomposites obtained by complexing palygorskite to lawsone and methyl orange. *Micropor. Mesopor. Mat.* 2026;403:114018. doi:10.1016/j.micromeso.2025.114018
  20. Hernandez J, Robb A, Servera S, Bedrosian N, Gomez O, Duca Z, Thomas MB, Tamae D, Fischhaber PL, Garrett SJ, Ward PA, Teprovich Jr JA. Synthesis and Characterization of Amorphous Lawsone Polymer Dots for Fluorescent Applications. *ACS Appl. Nano Mater.* 2023;6(22):2063951. doi:10.1021/acsnm.3c03229
  21. Shrivastava A, Gupta V. Methods for the determination of limit of detection and limit of quantitation of the analytical methods. *Chronicles Young Sci.* 2011;2 (1):21-5. doi:10.4103/2229-5186.79345
  22. Ohyashiki T, Kadoya A, Kushida K. The role of Fe<sup>3+</sup> on Fe<sup>2+</sup>-dependent lipid peroxidation in phospholipid liposomes. *Chem. Pharm. Bull.* 2002;50(2):203-7. doi:10.1248/cpb.50.203
  23. Gulcin İ, Alwaseel SH. Fe<sup>3+</sup> Reducing Power as the Most Common Assay for Understanding the Biological Functions of Antioxidants. *Processes.* 2025;13(5):1296. doi:10.3390/pr13051296
  24. Zhang L, Zhang M, You S, Ma D, Zhao J, Chen Z. Effect of Fe<sup>3+</sup> on the sludge properties and microbial community structure in a lab-scale A<sub>2</sub>O process. *Sci. of The Total Environ.* 2021;780(1):146505. doi:10.1016/j.scitotenv.2021.146505
  25. Wang T, Zeng LH, Li DL. A review on the methods for correcting the fluorescence inner-filter effect of fluorescence spectrum. *Appl. Spectrosc. Rev.* 2017;52:883-908. doi:10.1080/05704928.2017.1345758
  26. Lakowicz JR. Principles of Fluorescence Spectroscopy. 3rd ed. Springer New York: New York; 2006. 954 p.
  27. Shanmugaraj K, John SA. Inner filter effect based selective detection of picric acid in aqueous solution using green luminescent copper nanoclusters. *New J. Chem.* 2018;42:7223-9. doi:10.1039/c8nj00789f
  28. Li H, Fu B, Yang W, Ding L, Yang Y, Dong J, Wang F, Pan Q. A recyclable fluorescent probe for picric acid detection in water samples based on inner filter effect. *Spectrochim. Acta Mol. Biomol. Spectrosc.* 2020;226:117575. doi:10.1016/j.saa.2019.117575